Journal of Biomechanics 46 (2013) 832–836

Contents lists available at SciVerse ScienceDirect

Journal of Biomechanics

journal homepage: www.elsevier.com/locate/jbiomech
www.JBiomech.com

Short communication

# *In vitro* assessment of available coaptation area as a novel metric for the quantification of tricuspid valve coaptation

Joseph R. Dolensky [a], Lauren D.C. Casa [b], Andrew W. Siefert [a], Ajit P. Yoganathan [a,b,*]

[a] The Wallace H. Coulter Department of Biomedical Engineering, Georgia Institute of Technology and Emory University, Atlanta, GA 30332, United States
[b] The George W. Woodruff School of Mechanical Engineering, Georgia Institute of Technology, Atlanta, GA 30332, United States

ARTICLE INFO

*Article history:*
Accepted 29 November 2012

*Keywords:*
Tricuspid valve
Simulation
Functional tricuspid regurgitation
Imaging
Measurement technique

ABSTRACT

Tricuspid regurgitation (TR) is associated with increased mortality in patients undergoing mitral valve repair. In recent decades, TR has been addressed using annuloplasty concomitantly with mitral valve repair by some surgeons. However, repair efficacy and durability are often suboptimal. Increased understanding of tricuspid valve coaptation and the effects of pathological and repair conditions may be useful to inform future repair design. In the present study, we propose a two-dimensional *in vitro* technique, available coaptation area (ACA), to quantify the area of each tricuspid leaflet available for coaptation. Preliminary results showed that annular dilatation caused a significant ($p < 0.05$) decrease in anterior leaflet ACA ($0.92 \pm 0.18$ cm$^2$), and combined annular dilatation and papillary muscle (PM) displacement resulted in a significant decrease in posterior leaflet ACA ($0.87 \pm 0.15$ cm$^2$). Isolated PM displacement did not have a significant effect on ACA, and the septal leaflet showed no changed in ACA under the conditions tested. In addition to quantifying ACA, our technique allows for the detailed mapping of leaflet coaptation, which may be used to reveal specific sites of malcoaptation on each leaflet. Application of the ACA method in future studies may lead to the development of specialized tricuspid repair strategies and annuloplasty ring designs that target specific regions of the tricuspid valve based on underlying pathological conditions.



## 1. Introduction

Tricuspid regurgitation (TR) is associated with increased morbidity and mortality in a number of pathologies, including mitral valve disease, pulmonary hypertension, and congestive heart failure (Izumi et al., 2002; Koelling et al., 2002; Bustamante-Labarta et al., 2002). Functional TR is defined as a structurally normal tricuspid valve rendered incompetent due to ventricular alterations (Anyanwu et al., 2008). Rogers and Bolling (2009) note annular dilatation and right ventricular enlargement as the chief causes of TR, which is treated concurrently with mitral valve repair (Ghoreishi et al., 2011; Yoda et al., 2011).

Despite tricuspid valve (TV) annuloplasty, the most common treatment of TR, recurrent TR has been observed in patients presenting with a severely dilated right ventricle (Yoda et al., 2011). Previous investigations have proposed alternate surgical methods (Ghoreishi et al., 2011; Kappert et al., 2008; Choi et al., 2011) to improve the outcome of TV repair, yet the mechanism behind repair failure is unclear, and thus a greater understanding of TV coaptation under pathologic and repair conditions may lead to better repair designs.

To fully characterize leaflet coaptation for repair design, an areal measurement of coaptation is necessary. However, previous methods, such as coaptation length (CL) and residual leaflet length (RLL) (Lee et al., 2009; Spinner et al., 2011) provide only one-dimensional assessment of coaptation and therefore cannot identify specific sites of poor coaptation. The use of *in vitro* simulators to isolate geometric effects and quantify a broad range of leaflet characteristics within a highly-controlled experimental environment has the potential to provide useful data to inform such designs. To this end, the present study aims to demonstrate a new 2D *in vitro* measurement technique to quantify the available coaptation area (ACA).

## 2. Methods

### 2.1. Valve preparation and experimental set-up

Porcine hearts were acquired from a local abattoir, and TVs ($n=8$) with an annular area of 6 cm$^2$ were excised preserving their annular and subvalvular

* Corresponding author at: Georgia Institute of Technology and Emory University, The Wallace H. Coulter Department of Biomedical Engineering, 313 Ferst Dr., Atlanta, GA 30332-0100, United States. Tel.: +1 404 894 2849; fax: +1 404 894 4243.
*E-mail address:* ajit.yoganathan@bme.gatech.edu (A.P. Yoganathan).

0021-9290/$ - see front matter © 2013 Elsevier Ltd. All rights reserved.
http://dx.doi.org/10.1016/j.jbiomech.2012.11.054

anatomy. Using a previously described right heart simulator (Spinner et al., 2011), excised TVs were sutured to an adjustable annulus plate and PMs attached to positioning rods. Simulations were performed at 70 beats/min with a cardiac output of 5 L/min, transvalvular pressure of 40 mmHg. Saline was utilized as a blood analog which has been shown to be an appropriate fluid model (Jimenez et al., 2005; Spinner et al., 2011, 2012a, and others). Normal coaptation was simulated by positioning each of the PMs directly behind each commissure with the chordae taut during systole and inspected to verify coaptation characteristics described clinically (Carpentier et al., 2010). Flow and pressure (Fig. 1) were monitored with an electromagnetic flow probe (600 series, Carolina Medical Electronics, East Bend, NC) and static pressure transducers (Deltran® DPT-200, Utah Medical Products, Inc.; Midvale, UT) mounted in the right atrium and ventricle. After calibration, the flow probe was accurate to within 5 mL/min and the pressure transducer to within 1 mmHg over the full range.

The effect of annular dilatation was investigated by dilating the anterior and posterior segments of the tricuspid annulus to 1.4 times the normal annular area (6 $cm^2$) (Fig. 4A) (Carpentier et al., 2010). Simulated LV and RV dilatation were additionally studied by repositioning each of the PMs (Table 1, Fig. 4B and Fig. 4C).

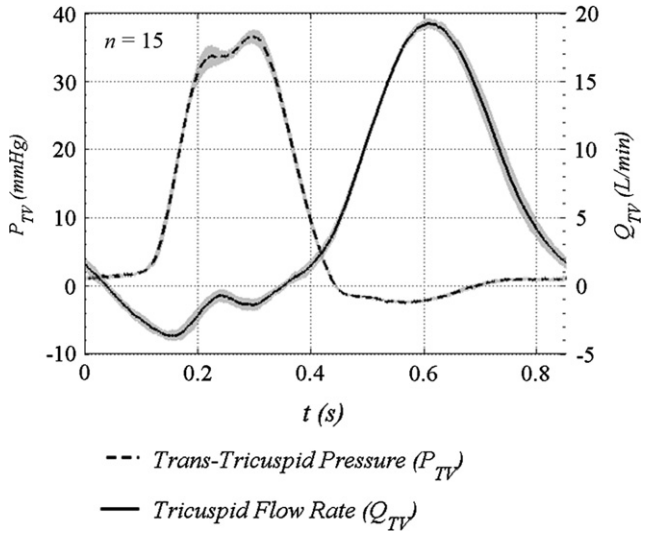


**Fig. 1.** Averaged transvalvular flow and pressure waveforms of the control condition measured by probes within the right heart simulator. Waveforms are the average of 15 cardiac cycles and the shaded region shows the mean ± standard deviation. The horizontal axis, *t*, is time in seconds.

**Table 1**
Papillary muscle positioning.

| Papillary muscle | PM displacement direction (mm) | | |
|---|---|---|---|
| | Septal | Anterior | Apical |
| Anterior | 0 | 10 | 10 |
| Posterior | 5 | 5 | 10 |
| Septal | 5 | 0 | 10 |

The PM displacement directions were ascertained from echocardiographic images of five patients (four normal volunteers and one with RV and LV dilatation and severe pulmonary hypertension). The patient with pulmonary hypertension was included because it is associated with TR and TR severity (Spinner et al., 2012b). The location of the PMs on the abnormal volunteer determined the PM displacement directions using the four normal volunteers as a reference. Similar to Spinner et al. (2011), the magnitude of PM displacement for the free wall PM (anterior) was 10 mm. Movements of 5 mm reflect the smaller changes in the PMs on the septal wall observed clinically as a result of concomitant LV–RV dilatation.

### 2.2. Coaptation area

Prior to each experiment, a $2 \times 2$ $mm^2$ grid of ink dots (Thermo Scientific, Pittsburg, PA) was applied to each TV leaflet and a reference image of the minimally stretched leaflet grid was recorded (Fig. 2A). During experimentation, the leaflet markers were imaged (at 30 fps) throughout the cardiac cycle using a camera placed perpendicular to the annular plane. The peak systolic frame of each condition was selected as the first frame after which the leaflets are stationary (Fig. 2B). In the peak systolic image, visible dots were identified and mapped to a matrix. ACA was calculated for each leaflet from the computed matrices using a custom MATLAB code (R2008bSV, The Math Works, Natick, MA) as the area (trapezoidal Riemann sum) of the visible dots subtracted from the area determined by the reference image. In this way, ACA represents the total amount of leaflet available for coaptation, shown as the shaded region in Fig. 2C.

### 2.3. Data analysis

Change in ACA from control was used as the endpoint of interest. All data was tested for normality using an Anderson–Darling test. A general linear model with a Tukey post-hoc test was used to determine statistical significance ($p < 0.05$). All analyses were completed using with Minitab (v. 16.1.0; Minitab, Inc.; State College, PA), and reported as a mean ± standard error.

## 3. Results

Isolated annular dilatation had a significant effect on the anterior leaflet, reducing the ACA by $-0.92 \pm 0.25$ $cm^2$ compared to normal (Fig. 3A). Annular dilatation alone did not significantly affect the posterior or septal leaflets. Isolated PM displacement did not significantly reduce the ACA of any leaflet. Annular dilatation and PM displacement did significantly reduce the anterior and posterior leaflets by $-0.97 \pm 0.18$ $cm^2$ and $-0.87 \pm 0.15$ $cm^2$ from normal, respectively (Fig. 3A and B).

## 4. Discussion

The present study aimed to develop an *in vitro* method to quantify the total TV leaflet ACA. Significant reductions in ACA due to annular dilatation can be explained by the greater distance between the leaflet bases as a direct result of increasing the annulus area (Fig. 4A). Although not significant in isolation, the outward PM displacement from the center of the ventricle, like annular dilatation, pulls the leaflets farther from each other, again

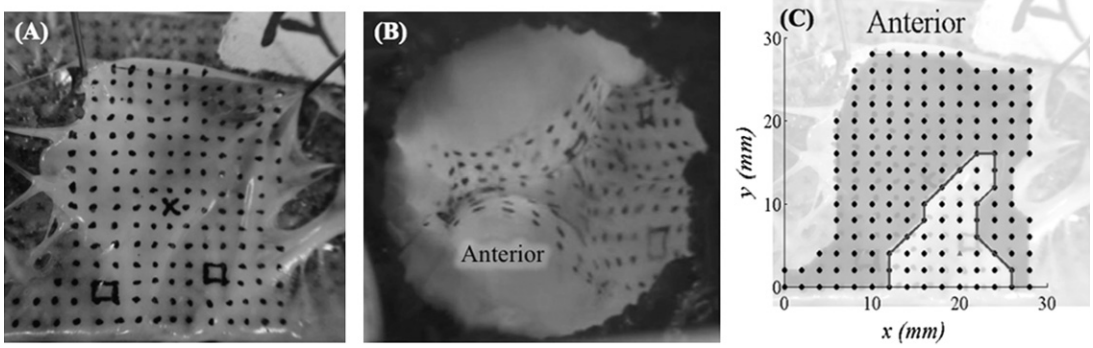


**Fig. 2.** Summary of ACA technique. (A) Reference image taken after leaflet is inked in with $2 \times 2$ $mm^2$ grid, (B) peak systolic image where visible dots are recorded, and (C) schematic of calculated ACA (shaded), white area represents visible dots in panel B.